European Journal of Medicinal Chemistry 62 (2013) 148–157

Contents lists available at SciVerse ScienceDirect

European Journal of Medicinal Chemistry

journal homepage: http://www.elsevier.com/locate/ejmech

Original article

Synthesis of derivatives of methyl rosmarinate and their inhibitory activities against matrix metalloproteinase-1 (MMP-1)

Hu Yuan [a,d,1], Weiqiang Lu [b,1], Liyan Wang [b], Lei Shan [a], Honglin Li [b], Jin Huang [b,*], Qingyan Sun [c,*], Weidong Zhang [a,d,**]

[a] Department of Phytochemistry, School of Pharmacy, Second Military Medical University, Shanghai 200433, China
[b] Shanghai Key Laboratory of Chemical Biology, State Key Laboratory of Bioreactor Engineering, School of Pharmacy, East China University of Science and Technology, Shanghai 200237, China
[c] Department of Organic Chemistry, School of Pharmacy, Second Military Medical University, Shanghai 200433, China
[d] School of Pharmacy, Shanghai Jiao Tong University, Shanghai 200240, China

ARTICLE INFO

Article history:
Received 9 June 2012
Received in revised form
27 September 2012
Accepted 28 September 2012
Available online 16 October 2012

Keywords:
MMP-1
Inhibitors
SAR

ABSTRACT

A series of MMP-1 inhibitors have been identified based upon a methyl rosmarinate scaffold using structure-based drug design methods. The best compound in the series showed an IC_{50} value of 0.4 μM. A docking study was conducted for compound (S)-**10n** in order to investigate its binding interactions with MMP-1. The structure–activity relationships (SAR) were also briefly discussed. Useful SAR was established which provides important guidelines for the design of future generations of potent inhibitors against MMP-1.

1. Introduction

The matrix metalloproteinases (MMPs) are a family of zinc-dependent endopeptidases that are involved in the degradation of all components of the extracellular matrix [1]. The implication of MMPs in a number of pathological processes has been reported, thus, they are considered to be important therapeutic targets for the treatment of a wide array of disease processes such as cancer, tumor metastasis, arthritis, and cardiovascular diseases, as well as wound healing [2–9]. MMPs have been classified on the basis of their substrate specificity into the five following classes: gelatinases (MMP-2 and MMP-9), collagenases (MMP-1, -8, -13), stromelysins (MMP-3, -10), membrane types (MMP-14, -16, -17), and other related enzymes such as matrilysin (MMP-7) [10,11].

Interstitial collagenase (MMP-1), discovered from a metamorphosing tadpole in 1962 by Gross and Lapiere [12], plays an important role in diverse physiologic processes such as growth, tissue morphogenesis, and wound repair [13–15]. Likewise, it seems to be implicated in a variety of human diseases including atherosclerosis, rheumatoid arthritis, pulmonary emphysema, and fibrotic disorders, suggesting that its inhibition or stimulation may open therapeutic avenues [16,17]. Last year, Paul Elkington's group found that MMP-1 may drive tissue destruction in immunopathology of Tuberculosis (TB) and represents a therapeutic target to limit immunopathology [18]. The major structural difference observed between MMP-1 and other MMP enzymes is the relative size and shape of the S1' pocket. MMP-1 is characterized by a short and narrow S1' pocket. Currently, there are only two well-defined structures of MMP-1 available in the PDB. These two forms mainly differ in the S1' pocket, which can be in a "closed" (low energy) or in an "open" (inhibitor induced) conformation [19–21] Fig. 1.

During the past decades, a variety of different structural classes of MMP-1 inhibitors have been discovered using structure-based design and combinatorial chemistry [22,23]. Some of these inhibitors showed promising pre-clinical results in various cancer models [24]. Broad spectrum MMP inhibitors **I** (marimastat) [25] and **II** (prinomastat) [26] were tested against cancers; MMP

* Corresponding authors. Tel./fax: +86 21 81871244.
** Corresponding author. Department of Phytochemistry, School of Pharmacy, Second Military Medical University, Shanghai 200433, China. Tel./fax: +86 21 81871244.
E-mail addresses: huangjin@ecust.edu.cn (J. Huang), sqy_2000@163.com (Q. Sun), wdzhangy@hotmail.com (W. Zhang).
[1] These authors contributed equally to this work.

0223-5234/$ – see front matter © 2012 Elsevier Masson SAS. All rights reserved.
http://dx.doi.org/10.1016/j.ejmech.2012.09.047

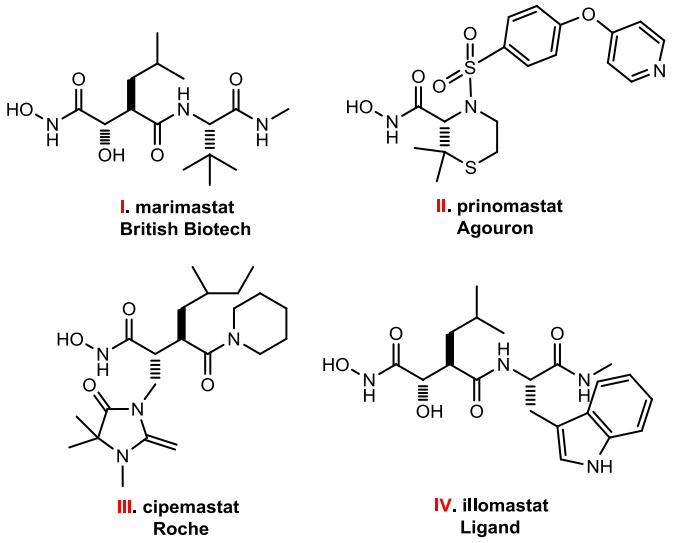

Fig. 1. Molecular structures of four broad spectrum MMP inhibitors tested in clinical trials.

inhibitors **III** (cipemastat) [27] and **IV** (ilomastat) [28] were tried in the clinics for inflammation. However, advanced clinical trials of these compounds failed for poor oral bioavailability, decreased potency in vivo and musculoskeletal side effects. Hence, developing new types of MMP-1 inhibitors is especially essential.

Our previous screening disclosed natural product methyl rosmarinate (**1**) as a MMP-1 inhibitor with an IC_{50} of 14.7 μM against MMP-1 (unpublished data). Specific interactions devised by molecular docking between **1** and MMP-1 are shown in Fig. 2A. The phenyl ring of the caffeic acid group inserts into the enzymes' hydrophobic domains (S1' pocket), which makes hydrophobic interaction with His218 and Tyr240. In addition, several polar interactions occur in the interactions between compound and the enzyme. The carbonyl group has a chelate bond with the zinc atom of the enzyme. Another carbonyl group in the middle of the compound makes ionic interactions with the polar nitrogen atom of Ala182. And the hydroxyl groups of the two terminal aryl rings which locate in compound make hydrogen bonds with the polar atoms of Ala234, Thr241 in S1' pocket and Asn180 in S3' pocket, respectively. Hence, when compound **1** is bound to MMP-1, the enzyme is inactivated resulting from high affinity between compound **1** and MMP-1.

To probe the SAR of the derivatives of methyl rosmarinate as MMP-1 inhibitors and exploit more potent MMP-1 inhibitors, we have investigated various replacements for the R_1, R_2, and R_3 groups according to the results of computer-aided drug design (Fig. 2B), which predicted that different substituent groups for R_1, R_2, and R_3 may make differences in activities of the compounds. Meanwhile, R_2 and R_3 groups seem to be particularly important to the potency because they chelate with zinc ion and make hydrophobic interactions with S1' pocket, while R_1 group may play a less important role. Consequently, we defined R_1 as hydroxyl group or methoxyl group, R_2 as ester group, carboxyl group or hydroxamate group, and R_3 as different hydrophobic groups to discuss the effects of different substituted groups for compounds' inhibitional activities against MMP-1 in this paper. We now describe the structure-based design, synthesis of inhibitors of MMP-1 that utilizes methyl rosmarinate as a scaffold.

2. Chemistry

All the target compounds were designed and synthesized via the routes shown in Scheme 1. Compound **4** from 3,4-dimethoxybenzaldehyde and N-acetyl glycine was employed as

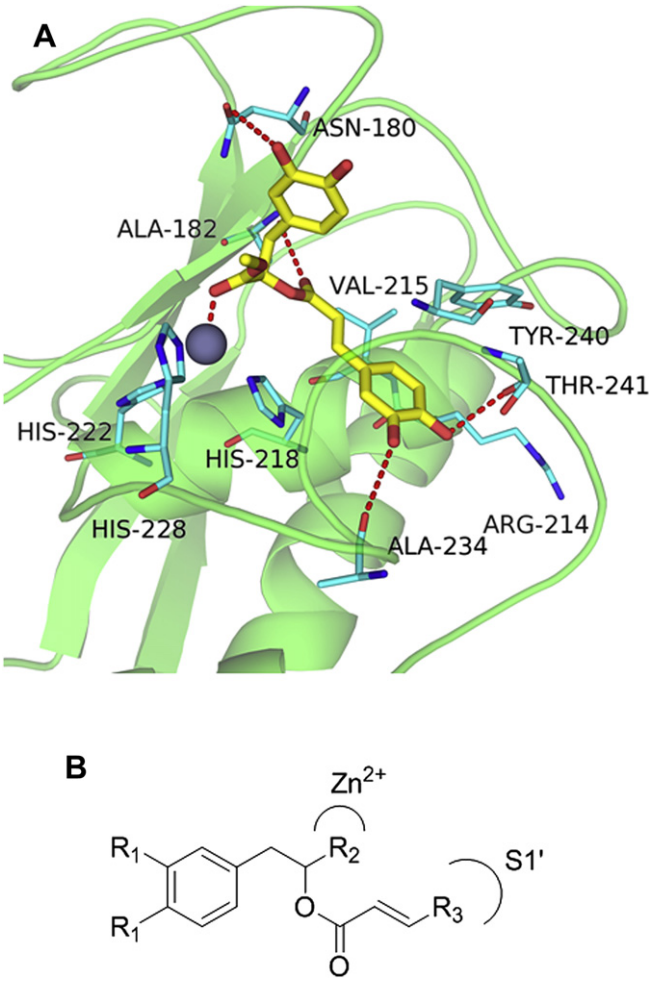

Fig. 2. (A) Ligand interaction diagrams for **1**, an inhibitor with a ZBG bound to MMP-1. The compound is represented by the yellow sticks. The amino residues are represented by the cyan lines. The zinc ion is represented by grey sphere. The MMP-1's tertiary structure is represented by the green cartoon. (B) Scaffold based on methyl rosmarinate. R_1, R_2, and R_3 groups were supposed to be replaced by different groups. (For interpretation of the references to colour in this figure legend, the reader is referred to the web version of this article.)

the first step. Further treatment with 3 M hydrochloric acid converted **4** into hydroxycinnamic acid **5** [29,30], and **5** was hydrogenated to the corresponding unstable lactic acid **6**, which was transformed to the allyl ester **7a** and methyl ester **7b** by reaction with allyl alcohol and methanol, respectively, followed by esterification (EDCI method) of allyl ester and methyl ester at the free alcoholic function with cinnamic acid (Scheme 1).

Compound **9q** was deprotected by TBAF in THF to afford **9q′** in a excellent yield (See Supporting information). The allyl esters **9a**–**k** and **9m**–**q′** were deprotected by catalytic amounts of $Pd(PPh_3)_4$ and morpholine following the Kunz–Waldmann procedure [31] to give substitutional rosmarinic acids **10a**–**p**, followed by condensation with hydroxylamine hydrochloride which afforded compounds **11f**, **11i**, **11j**, and **11n**–**p**.

The derivatives of cinnamic acids **8j** and **8n**–**q** were prepared conveniently from 3,4-dihydroxy cinnamic acid, p-hydroxy cinnamic acid by O-allylation and subsequent hydrolysis of the esters or Knoevenagel condensation of aldehydes (**12o**, **12p**) with malonic acid (See Supporting information). Completion of the synthesis required removal of four ether methyl groups to arrive at rosmarinic acid (**2**, See Supporting information). The deprotection of pentamethyl rosmarinic acid was studied, and it was found that

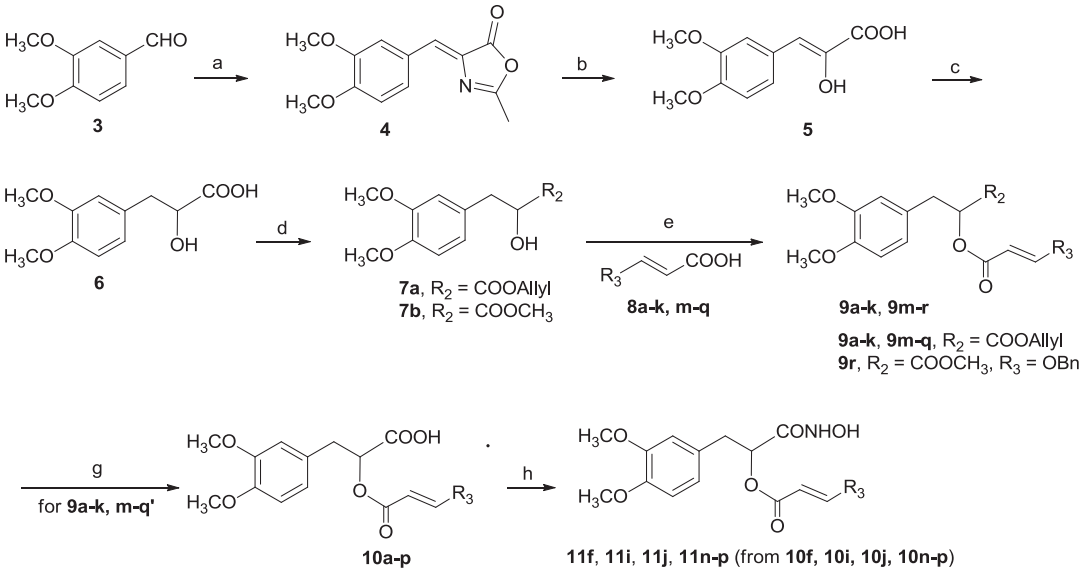

Reagents: a) NaOAc, Ac_2O, $AcHNCH_2COOH$; b) 3 M HCl; c) $NaBH_4$; d) p-TsOH, allyl alcohol or methanol, toluene; e) EDCI, DMAP, CH_2Cl_2; f) TBAF, THF; g) $Pd(PPh_3)_4$, morpholine, THF; h) DCC, DMAP, CH_2Cl_2, $NH_2OH{\cdot}HCl$.

Scheme 1. Synthetic route of target compounds.

several conditions gave only decomposition products or selective deprotection products (Table 1), which is difficult to separate by crystallization or column chromatography. Using Brossi's [32] conditions, in which iodotrimethylsilane (TMSI) and quinoline are precomplexed, pentamethyl rosmarinic acid was converted back to rosmarinic acid in 56% yield.

3. Results and discussion

All final compounds were tested in vitro, with a fluorometric assay on purified enzymes, for their abilities to inhibit MMP-1. Data obtained are shown in Table 2. Our approach focused on a series of derivatives beginning with the lead compound methyl rosmarinate (**1**), giving IC_{50} of 14.7 μM against MMP-1.

Firstly, our approach focused on a series of derivatives beginning with the lead compound methyl rosmarinate (**1**) with changing the R_2 group. Compound **2** was more potent than its predecessor **1**. As can be seen from the docking result (Fig. 3A), this activity difference was likely caused by the ZBG (R_2), which was the only structural difference between **2** and its predecessor **1**. The ZBG is carboxyl for **2** and ester for its predecessor **1**, respectively. Both of these two groups could chelate with zinc ion at catalytic activity center of the enzyme. However, the carboxyl group seemed to be a more potent ZBG than ester ($COOCH_3$) as shown in the activity order of **2** and its predecessor **1**, which was confirmed again by sharp decrease in activities after conversion from carboxyl group (**10c**, **10e**, **10f**, **10h**, and **10j**) to corresponding ester (**9c**, **9e**, **9f**, **9h**, and **9r**). Moreover, considering the high affinity of the hydroxamate moiety for zinc ion relative to other coordinating moieties [33], a series of hydroxamates (**11f**, **11i**, **11j**, and **11n**–**p**) were prepared to improve the activities of these ligands by allowing for a good interaction with the ZBGs in R_2 position. The results showed that compounds **11f**, **11i**, **11j**, and **11n**–**p** were more potent than their predecessors **10f**, **10i**, **10j**, and **10n**–**p**. These activity differences were likely caused by the ZBGs (R_2), which were the only structural difference between **11f**, **11i**, **11j**, and **11n**–**p** and their predecessors. The ZBG was hydroxamate (CONHOH) for **11f**, **11i**, **11j**, and **11n**–**p** and carboxyl for their predecessors. Therefore, the hydroxamate group was a more potent ZBG than carboxyl group as shown in the activity order of **11f**, **11i**, **11j**, and **11n**–**p** and their predecessors.

Next, R_1 group was altered by hydroxyl group and methoxyl group. Among compounds **2** and **10l**, R_2 and R_3 groups were fixed as carboxyl and 3,4-dihydroxyphenyl, respectively. For compound **10l**, R_1 group was methoxyl, provided a 1.5-fold decrease in the inhibitory activity compared to compound **2**, which indicated that methoxyl substitution at R_1 position was less favorable than the hydroxyl substitution. This might be attributed to the hydroxyl group, which has stronger hydrophilic interaction than the methoxyl group, was more favorable for binding the site of a solvent exposed area (Fig. 3).

Finally, we turned our attention to understand the R_3 group's effects on MMP-1. It was altered by various substituted phenyls. Among compounds **10a**–**c**, **10h**, **10k**, **10m**, **10o**, and **10p**, R_1 and R_2 groups were fixed as methoxyl and carboxyl, respectively, and R_3

Table 1
Demethylation of pentamethyl rosmarinic acid (**10m**).

Entry	Reagents and conditions	Yield/%
1	BBr_3, CH_2Cl_2, −50 °C	Ester cleavage
2	46% HBr, TBAB, reflux	Ester cleavage
3	$AlCl_3$, $SHCH_2CH_2SH$, CH_2Cl_2, 25 °C	Decomposition
4	$BF_3{\cdot}Et_2O$, $SHCH_2CH_2SH$, 25 °C	Decomposition
5	Pyridine hydrochloride, 180 °C/N_2	Decomposition
6	$AlCl_3$, CH_2Cl_2, 25 °C	Partial deprotection
7	Me_3SiI, $CHCl_3$, r.t./N_2	<5
8	Me_3SiI, quinoline, 4 h, 100 °C	<5
9	Me_3SiI, quinoline, 4 h, 180 °C	56

Table 2
Evaluation of synthesized compounds for their inhibitory activity towards MMP-1.

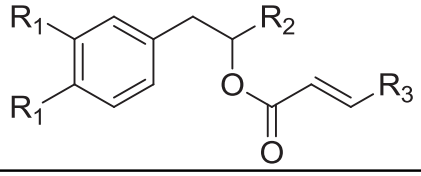

Compound	R_1	R_2	R_3	Inhibition[a] (%)	IC_{50} (μM)
1	OH	COOMe	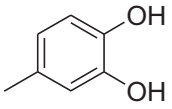	58.6	14.7
2	OH	COOH	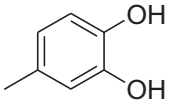	68.6	5.6
10a	OMe	COOH	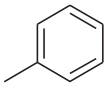	28	53.7
10b	OMe	COOH	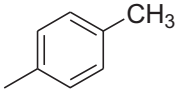	10.3	>100
10c	OMe	COOH	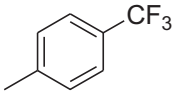	25.8	38.9
10d	OMe	COOH	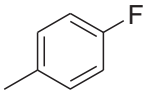	22.9	41.7
10e	OMe	COOH	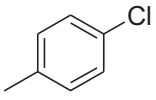	40.6	42.6
10f	OMe	COOH	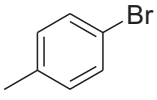	73.1	10.7
10g	OMe	COOH	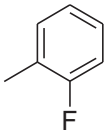	33.2	34.7
10h	OMe	COOH	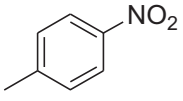	29.8	38.5
10i	OMe	COOH	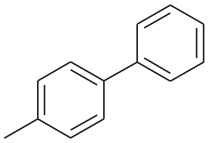	55.7	8.6
10j	OMe	COOH	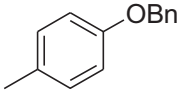	87.9	8.9

Table 2 (*continued*)

Compound	R_1	R_2	R_3	Inhibition[a] (%)	IC_{50} (μM)
10k	OMe	COOH	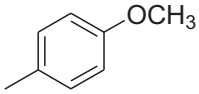	0	>100
10l	OMe	COOH	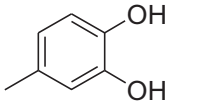	43.2	13.7
10m	OMe	COOH	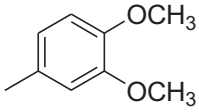	21.3	>100
10n	OMe	COOH	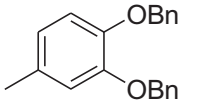	86.6	2.5
10o	OMe	COOH	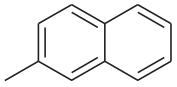	0.1	>100
10p	OMe	COOH	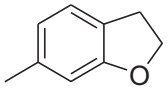	0.3	>100
11f	OMe	CONHOH	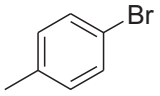	56.8	7.6
11i	OMe	CONHOH	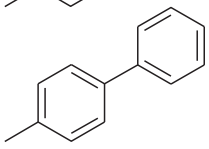	85.4	5.5
11j	OMe	CONHOH	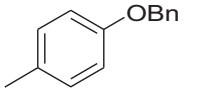	87.2	3.6
11n	OMe	CONHOH	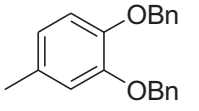	100	4.2
11o	OMe	CONHOH	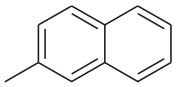	65	6.8
11p	OMe	CONHOH	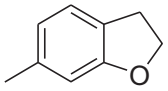	47.9	10.6
9c	OMe	COOAllyl	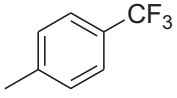	1.8	>100
9e	OMe	COOAllyl	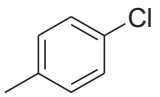	0	>100

(*continued on next page*)

Table 2 (*continued*)

Compound	R_1	R_2	R_3	Inhibition[a] (%)	IC_{50} (μM)
9f	OMe	COOAllyl	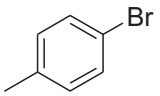	14.2	>100
9h	OMe	COOAllyl	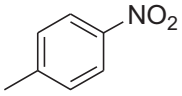	0	>100
9r	OMe	COOMe	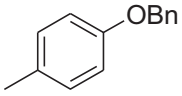	1.7	>100
(**R**)-**10n**	OMe	COOH	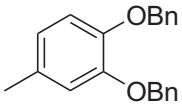	100	0.4
(**S**)-**10n**	OMe	COOH	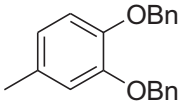	100	0.8

[a] Measured at 10 μM.

group was altered as various substituted phenyls. So the differences in the inhibitory activities of these compounds were likely caused by various R_3 groups. For compound **10a**, R_3 group was phenyl, provided a 3-fold decrease in the inhibitory activity compared to compound **10l**. For compounds **10b**, **10k**, **10m**, **10o**, and **10p**, R_3 group were 4-methylphenyl, 4-methoxyphenyl, 3,4-dimethoxyphenyl, naphthyl, and 2,3-dihydrobenzofuran, respectively, showed no inhibitory activities against MMP-1. For compound **10c** and **10h**, R_3 group were 4-trifluoromethylpheny and 4-nitrophenyl, respectively, each compound demonstrated a 1.8-fold decrease in the inhibitory activity compared to compound **10l**. These results suggested that small hydrophobic substituent groups on aromatic ring impaired affinity, which might be attributed to the small hydrophobic groups were unfavorable to the accommodation with the enzymes' hydrophobic domain (S1' pocket). Comparing compounds with halogen-substitution at the para-position or ortho-position in the aromatic ring (**10d**–**g**), it seemed that the increased bulk of halogen substituents leads to improved activities, suggesting there is a space requirement in the binding pocket to accommodate the suitable substituents. Among compounds **10i**, **10j**, and **10n**, R_1 and R_2 groups were fixed as methoxyl and carboxyl, respectively, and R_3 group was altered as various substituted phenyls. So the differences in the inhibitory activities of these compounds were likely caused by various R_3 groups. Compound **10n** displayed the highest affinity (IC_{50} = 2.5 μM), compound **10i** and **10j** presented similar activities, suggesting long and bulky hydrophobic substituents on aromatic ring improved affinities, which might be attributed to the long and bulky hydrophobic groups were favorable to the accommodation with S1' pocket because they were able to induce the "open" conformational change (long and bulky hydrophobic substituent groups at R_3 position required Arg 214 to adopt a new position (Fig. 4), creating a larger, open S1' pocket).

In order to rationalize the affinities observed for our inhibitors, the binding modes of compound (S)-**10n** (the pure R-enantiomer and S-enantiomer of **10n** were accomplished using chiral chromatography) within the MMP-1 were studied by computational docking method. Several important features of possible

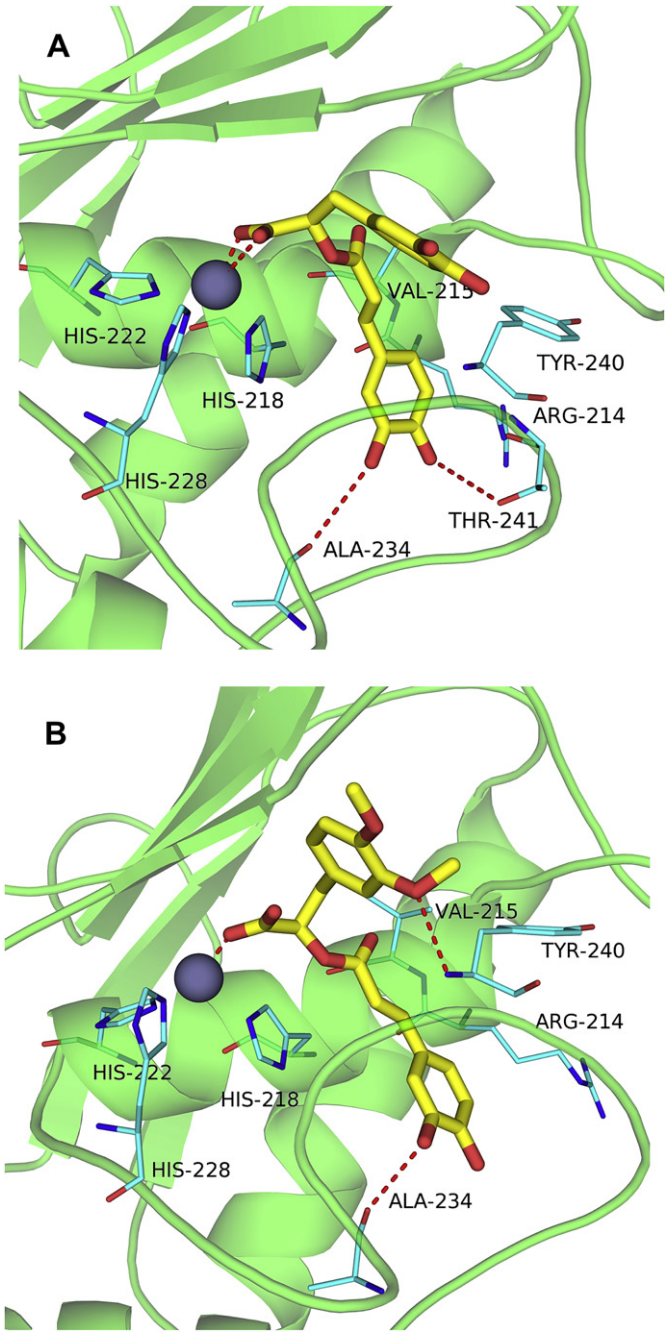

Fig. 3. Docking of compound **2** (A) and **10l** (B) into MMP-1. The compound is represented by the yellow sticks. The amino residues are represented by the cyan lines. The zinc ion is represented by grey sphere. The MMP-1's tertiary structure is represented by the green cartoon. (For interpretation of the references to colour in this figure legend, the reader is referred to the web version of this article.)

interactions can be derived from the predicted binding mode of (S)-**10n**. According to the Fig. 4, we can find that the compounds can occupy three subpockets (S1, S1' and S3') of MMP-1, and form chelate bonds through the carboxyl group and the zinc ion. Moreover, the compound (S)-**10n** is also stabilized by hydrophobic interactions in the S1'and S3' pocket. In the S1' pocket, the 4-(benzyloxyl)phenyl of the compound makes hydrophobic contacts with residues Val 215, Arg 214 and His 218, while the 3-(benzyloxyl) phenyl makes hydrophobic contacts with residues Tyr-240 and Tyr-210 in the S3' pocket. It is worth noticing that the group in para-position of the benzene ring embedded in the S1' pocket. When it

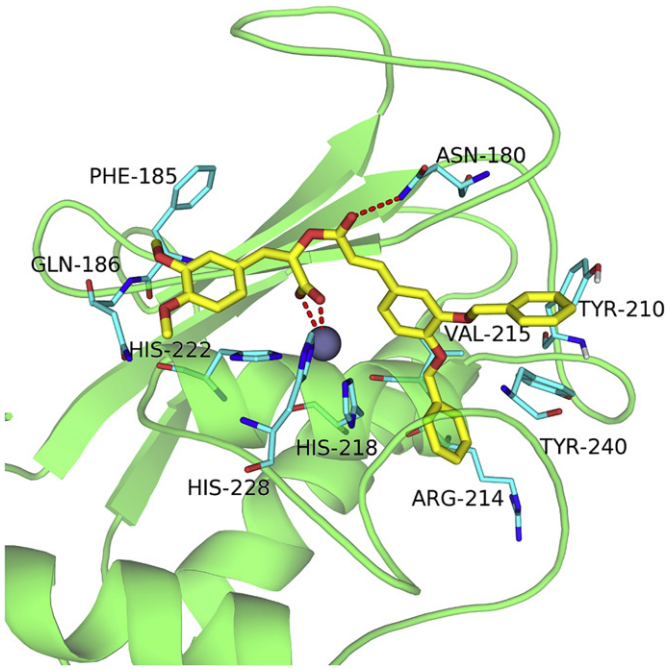

Fig. 4. The predicted binding mode of the compound (**S**)-**10n** against the MMP-1. The compound is represented by the yellow sticks. The amino residues are represented by the cyan lines. The zinc ion is represented by grey sphere. The MMP-1's tertiary structure is represented by the green cartoon. (For interpretation of the references to colour in this figure legend, the reader is referred to the web version of this article.)

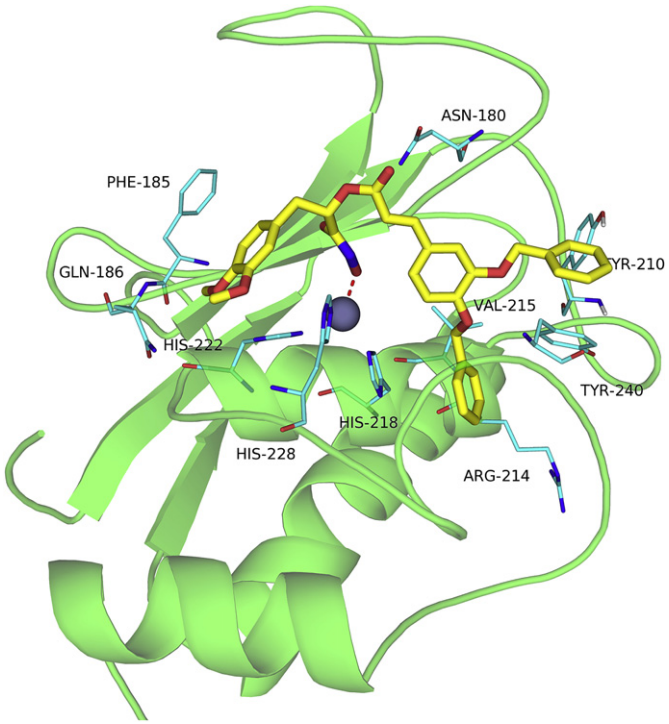

Fig. 5. The predicted binding mode of (**S**)-**11n** aganst the MMP-1. The compound is represented by the yellow sticks. The amino residues are represented by the cyan lines. The zinc ion is represented by grey sphere. The MMP-1's tertiary structure is represented by the green cartoon. (For interpretation of the references to colour in this figure legend, the reader is referred to the web version of this article.)

Table 3
Evaluation of R(−)10n and S(−)10n for their inhibitory activities towards MMPs.

Compound	IC_{50} (μM)					
	MMP-1	MMP-2	MMP-3	MMP-9	MMP-12	MMP-13
(**R**)-**10n**	0.4	3.2	4.0	6.7	2.1	4.5
(**S**)-**10n**	0.8	3.0	3.4	6.0	2.3	5.4

was replaced with other small hydrophobic groups, such as 4-methoxyphenyl (**10k**), 4-trifluoromethylphenyl (**10c**) and 4-nitrophenyl (**10h**), the inhibitory activity would decrease. It indicated that the hydrophobic contact in the S1' pocket is important for the inhibitory activity. Compared carboxylic acids (**10f**, **10i**, **10j**, **10n**, **10o** and **10p**) and hydroxamates (**11f**, **11i**, **11j**, **11n**, **11o** and **11p**), it was found that the exception is compound **10n** that gives the best results much better than the parent **11n**. The docking study shows that the compound (S)-**11n** has a similar binding pose with the compound (S)-**10n**, but there is a difference at the chelated group: the hydroxamate group of compound (S)-**11n** forms a monodentate chelating replaced the bidentate chelating of compound (S)-**10n**, which decrease the binding affinity of (S)-**10n** (Fig. 5). And this phenomenon only appears for compound **11n**, it is presumed that the long and bulky R_3 group pushes the chelate group hydroxamate away from the zinc atom, which might cause the activity of the compound (S)-**11n** poorer than compound (S)-**10n**. Further up along the active pocket, the linker groups in the middle of the inhibitor almost wrap around the zinc atom and the carbonyl group of the linker groups forms hydrogen bonds with the nitrogen of Asn-180. The other terminal extends toward the S1 pockets: the 3,4-dimethoxyphenyl makes an interaction with Phe-185 and Gln-186 by hydrophobic contacts. The cupped inhibitor conformation predicted fits the shape and size of the catalytic position of the MMP-1 well, so it makes the compound combine with the enzyme closely, which is consistent with the high potency against MMP-1.

(R)-**10n** and (S)-**10n** were also tested for their inhibitory activities towards MMP-1, -2, -3, -9, -12, and -13 (Table 3). The activity of **10n** against MMP-1 is almost 5–10-fold better than for the other MMPs. Although the selectivity toward MMP-1 versus other MMPs was not satisfying, the result encourages us to further design selective MMP-1 inhibitors using **10n** as a lead compound which would be reported later.

In a word, the binding mode of the most potent compound with MMP-1 was proposed as follows: (1) the hydroxamate or carboxyl group on the scaffold (R_2) chelates the active site zinc ion; (2) at least one functional group on the scaffold that provides a hydrogen bond interaction with the enzyme sidechain; (3) bulky hydrophobic substituents on aromatic ring (R_3) accommodate with the enzymes' hydrophobic domains (S1' pocket). The above binding mode information encouraged us to further design rosmarinic acid scaffold-based selective MMP-1 inhibitors, which will be reported later.

4. Conclusions

In summary, we have developed a new series of rosmarinic acid derivatives as MMP-1 inhibitors, in which the compound (R)-**10n** was the most potent candidate. SAR studies indicated that hydrophilic group R_1, strong electronegative group R_2, and bulky hydrophobic group R_3 at scaffold favored the inhibitory activity against MMP-1. A docking study of the most interesting compound allowed the understanding of its binding interactions with MMP-1, thus suggesting the basis of its activity profile. This feature may provide us a critical point for further chemical modification on rosmarinic acid derivatives so as to exploit more potent MMP-1 inhibitors.

5. Experimental section

5.1. Chemistry

Nuclear magnetic resonance (NMR) spectra were recorded using TMS as the internal standard in DMSO-d_6, MeOD or $CDCl_3$ with a Bruker BioSpin GmbH spectrometer at 300 MHz. When peak multiplicities are reported, the following abbreviations are used: s = singlet, d = doublet, t = triplet, m = multiplet, br = broadened, dd = doublet of doublets, dt = doublet of triplets; ESI-MS was recorded on Agilent 1100 LC/MSD (70 ev) spectrometers. HRMS was recorded on a Waters Q-Tof micro. Melting points (m.p.) were determined by microscope melting point apparatus with aromatic temperature control system (XT4A). THF was distilled from sodium/benzophenone ketyl. Dichloromethane was distilled over CaH_2. All other reagents and starting materials were purchased and used as received (Aldrich, TCI, Adamas). Reactions were monitored by analytical TLC using silica gel 60 F254 plates and spots were visualized by UV light irradiation (254 nm). Flash column chromatography was performed by using silica gel (200–300 mesh). All test compounds showed ≥95% purity as determined by combustion analysis or by high-performance liquid chromatography (HPLC). HPLC conditions were as follows: CHIRALPAK ADH, 4.6 mm × 250 mm, 5% → 90% CH_3CN/MeOH/0.1% acetic acid, 15 min run, flow rate 0.7 mL/min, UV detection (λ = 220 nm).

5.1.1. Typical reaction procedure for compounds (**10a**–**p**)

A solution of the allyl esters (**9a**–**k** or **9m**–**q**′, 0.03 mmol) in tetrahydrofuran (10 mL) was stirred in an argon atmosphere at ambient temperature, $Pd(PPh_3)_4$ (0.002 mmol) and morpholine (0.6 mmol) were added subsequently. After 30 min the solvent was evaporated, and the residue was taken up in CH_2Cl_2 (50 mL). The resulting solution was extracted three times with 2 N HC1 (10 mL), dried over $MgSO_4$, and concentrated in vacuo. The desired acid was obtained after column purification using petroleum ether, ethyl acetate and acetic acid (33:66:1) as the mobile phase eluent.

5.1.2. (E)-2-(cinnamoyloxy)-3-(3,4-dimethoxyphenyl) propanoic acid (**10a**)

Yellow amorphous solid (83% yield); ^{1}H NMR ($CDCl_3$, 300 MHz): δ (ppm), 3.11–3.28 (m, 2H, CH_2), 3.85 (s, 3H, OCH_3), 3.86 (s, 3H, OCH_3), 5.32–5.39 (m, 1H, CH), 6.46 (d, J = 15.9 Hz, 1H, CH), 6.79–6.86 (m, 3H, ArH), 7.38–7.52 (m, 5H, ArH), 7.71 (d, J = 15.9 Hz, 1H, CH); ^{13}C NMR ($CDCl_3$, 75 MHz): δ (ppm), 37.1, 55.9, 73.3, 111.2, 112.7, 119.5, 121.5, 125.9, 128.8, 130.9, 132.2, 137.7, 143.7, 148.1, 148.7, 165.9, 167.7; ESI-MS: m/z 379.1 $[M + Na]^+$, 355.0 $[M - H]^-$; HRMS (ESI): m/z calcd for $C_{20}H_{20}O_6Na$ $[M + Na]^+$: 379.1158, found 379.1139.

5.1.3. (E)-3-(3,4-dimethoxyphenyl)-2-(3-p-tolylacryloyloxy) propanoic acid (**10b**)

White amorphous solid (85% yield); ^{1}H NMR ($CDCl_3$, 300 MHz): δ (ppm), 2.36 (s, 3H, CH_3), 3.09–3.26 (m, 2H, CH_2), 3.84 (s, 3H, OCH_3), 3.85 (s, 3H, OCH_3), 5.33 (m, 1H, CH), 6.40 (d, J = 15.9 Hz, 1H, CH), 6.77–6.85 (m, 3H, ArH), 7.17 (d, J = 7.8 Hz, 2H, ArH), 7.39 (d, J = 8.1 Hz, 2H, ArH), 7.67 (d, J = 15.9 Hz, 1H, CH); ^{13}C NMR ($CDCl_3$, 75 MHz): δ (ppm), 21.3, 37.2, 55.8, 73.0, 111.2, 112.7, 118.9, 121.7, 128.5, 128.8, 129.8, 131.6, 140.9, 145.6, 148.4, 148.9, 166.6, 168.3; ESI-MS: m/z 393.2 $[M + Na]^+$, 369.0 $[M - H]^-$; HRMS (ESI): m/z calcd for $C_{21}H_{22}O_6Na$ $[M + Na]^+$: 393.1314, found 393.1332.

5.1.4. (E)-3-(3,4-dimethoxyphenyl)-2-(3-(4-(trifluoromethyl) phenyl) acryloyloxy) propanoic acid (**10c**)

White amorphous solid (78% yield); ^{1}H NMR ($CDCl_3$, 300 MHz): δ (ppm), 3.08–3.29 (m, 2H, CH_2), 3.83 (s, 3H, OCH_3), 3.84 (s, 3H, OCH_3), 5.35 (s, 1H, CH), 6.52 (d, J = 15.9 Hz, 1H, CH), 6.78–6.86 (m, 3H, ArH), 7.44–7.73 (m, 5H, CH and ArH); ^{13}C NMR ($CDCl_3$, 75 MHz): δ (ppm), 37.0, 55.8, 73.6, 111.2, 112.6, 119.7, 121.5, 125.9, 128.3, 128.7, 130.9, 132.1, 132.2, 137.5, 143.9, 148.0, 148.8, 165.7, 167.8; ESI-MS: m/z 447.1 $[M + Na]^+$, 423.0 $[M - H]^-$; HRMS (ESI): m/z calcd for $C_{21}H_{19}F_3O_6Na$ $[M + Na]^+$: 447.1031, found 447.1053.

5.1.5. (E)-3-(3,4-dimethoxyphenyl)-2-(3-(4-fluorophenyl) acryloyloxy) propanoic acid (**10d**)

White amorphous solid (76% yield); ^{1}H NMR ($CDCl_3$, 300 MHz): δ (ppm), 3.08–3.28 (m, 2H, CH_2), 3.84 (s, 3H, OCH_3), 3.85 (s, 3H, OCH_3), 5.34 (s, 1H, CH), 6.36 (d, J = 15.9 Hz, 1H, CH), 6.78–7.57 (m, 7H, ArH), 7.65 (d, J = 15.9 Hz, 1H, CH); ^{13}C NMR ($CDCl_3$, 75 MHz): δ (ppm), 37.1, 55.9, 73.5, 111.1, 112.5, 119.8, 121.9, 125.3, 128.2, 131.3, 132.8, 137.9, 144.3, 148.6, 148.9, 166.2, 167.9; ESI-MS: m/z 397.2 $[M + Na]^+$, 372.9 $[M - H]^-$; HRMS (ESI): m/z calcd for $C_{20}H_{19}FO_6Na$ $[M + Na]^+$: 397.1063, found 397.1054.

5.1.6. (E)-2-(3-(4-chlorophenyl) acryloyloxy)-3-(3,4-dimethoxyphenyl) propanoic acid (**10e**)

White amorphous solid (88% yield); ^{1}H NMR ($CDCl_3$, 300 MHz): δ (ppm), 3.11–3.28 (m, 2H, CH_2), 3.85 (s, 3H, OCH_3), 3.86 (s, 3H, OCH_3), 5.36 (m, 1H, CH), 6.42 (d, J = 15.9 Hz, 1H, CH), 6.78–6.85 (m, 3H, ArH), 7.39 (dd, J = 24.9, 8.4 Hz, 4H, ArH), 7.64 (d, J = 15.9 Hz, 1H, CH); ^{13}C NMR ($CDCl_3$, 75 MHz): δ (ppm), 37.1, 55.9, 73.0, 111.2, 112.7, 118.7, 121.9, 128.3, 129.7, 132.4, 136.7, 144.4, 148.3, 148.9, 165.7, 167.4; ESI-MS: m/z 413.1 $[M + Na]^+$, 388.9 $[M - H]^-$; HRMS (ESI): m/z calcd for $C_{20}H_{19}ClO_6Na$ $[M + Na]^+$: 413.0768, found 413.0787.

5.1.7. (E)-2-(3-(4-bromophenyl) acryloyloxy)-3-(3,4-dimethoxyphenyl) propanoic acid (**10f**)

White amorphous solid (82% yield); ^{1}H NMR ($CDCl_3$, 300 MHz): δ (ppm), 3.07–3.26 (m, 2H, CH_2), 3.84 (s, 3H, OCH_3), 3.85 (s, 3H, OCH_3), 5.53 (brs, 1H, CH), 6.38 (d, J = 15.9 Hz, 1H, CH), 6.71–6.83 (m, 3H, ArH), 7.35 (d, J = 8.7 Hz, 2H, ArH), 7.53 (d, J = 8.1 Hz, 2H, ArH), 7.61 (d, J = 15.9 Hz, 1H, CH); ^{13}C NMR ($CDCl_3$, 75 MHz): δ (ppm), 37.1, 55.9, 72.8, 111.2, 112.7, 117.7, 121.7, 125.4, 129.6, 132.2, 132.9, 144.5, 145.7, 148.2, 148.9, 165.4, 166.6; ESI-MS: m/z 458.2 $[M + Na]^+$, 433.1 $[M - H]^-$, 869.0 $[2M - H]^-$; HRMS (ESI): m/z calcd for $C_{20}H_{19}BrO_6Na$ $[M + Na]^+$: 457.0263, found 457.0246.

5.1.8. (E)-3-(3,4-dimethoxyphenyl)-2-(3-(2-fluorophenyl) acryloyloxy) propanoic acid (**10g**)

White amorphous solid (81% yield); ^{1}H NMR ($CDCl_3$, 300 MHz): δ (ppm), 3.11–3.27 (m, 2H, CH_2), 3.83 (s, 3H, OCH_3), 3.85 (s, 3H, OCH_3), 5.23 (brs, 1H, CH), 6.55 (d, J = 16.2 Hz, 1H, CH), 6.84–7.50 (m, 7H, ArH), 7.80 (d, J = 15.9 Hz, 1H, CH); ^{13}C NMR ($CDCl_3$, 75 MHz): δ (ppm), 37.0, 55.9, 73.1, 111.2, 112.7, 116.4, 118.8, 119.5, 121.5, 124.5, 128.3, 129.5, 131.4, 132.0, 148.1, 148.9, 165.7, 168.0; ESI-MS: m/z 397.2 $[M + Na]^+$, 372.9 $[M - H]^-$; HRMS (ESI): m/z calcd for $C_{20}H_{19}FO_6Na$ $[M + Na]^+$: 397.1063, found 397.1051.

5.1.9. (E)-3-(3,4-dimethoxyphenyl)-2-(3-(4-nitrophenyl) acryloyloxy) propanoic acid (**10h**)

Yellow amorphous solid (83% yield); ^{1}H NMR ($CDCl_3$, 300 MHz): δ (ppm), 3.12–3.26 (m, 2H, CH_2), 3.86 (s, 3H, OCH_3), 3.87 (s, 3H, OCH_3), 5.35–5.43 (m, 1H, CH), 6.58 (d, J = 16.2 Hz, 1H, CH), 6.77–6.85 (m, 3H, ArH), 7.66 (d, J = 8.7 Hz, 2H, ArH), 7.72 (d, J = 16.2 Hz, 1H, CH), 8.23–8.26 (d, J = 8.7 Hz, 2H, ArH); ^{13}C NMR ($CDCl_3$, 75 MHz): δ (ppm), 37.1, 55.9, 73.2, 111.2, 112.6, 118.9, 121.3, 124.2, 128.8, 131.3, 140.3, 143.5, 148.3, 148.7, 148.9, 165.5, 168.9; ESI-MS: m/z 424.1 $[M + Na]^+$, 400.0 $[M - H]^-$; HRMS (ESI): m/z calcd for $C_{20}H_{19}NO_8Na$ $[M + Na]^+$: 424.1008, found 424.1023.

5.1.10. (E)-3-(3,4-dimethoxyphenyl)-2-(3-(4-phenylphenyl) acryloyloxy) propanoic acid (**10i**)

White amorphous solid (79% yield); ^{1}H NMR ($CDCl_3$, 300 MHz): δ (ppm), 3.08–3.20 (m, 2H, CH_2), 3.85 (s, 3H, OCH_3), 3.86 (s, 3H,

OCH_3), 5.53 (brs, 1H, CH), 6.46 (d, J = 15.9 Hz, 1H, CH), 6.75–7.62 (m, 12H, ArH), 7.73 (d, J = 15.9 Hz, 1H, CH); ^{13}C NMR ($CDCl_3$, 75 MHz): δ (ppm), 36.9, 55.9, 73.3, 111.3, 112.6, 116.6, 121.5, 127.0, 127.6, 127.9, 128.2, 128.7, 128.9, 133.0, 140.0, 143.4, 145.8, 148,2, 148.9, 166,2, 168.0; ESI-MS: m/z 455.2 $[M + Na]^+$, 431.1 $[M - H]^-$; HRMS (ESI): m/z calcd for $C_{26}H_{24}O_6$ Na $[M + Na]^+$: 455.1471, found 455.1452.

*5.1.11. (E)-2-(3-(4-(benzyloxy) phenyl) acryloyloxy)-3-(3,4-dimethoxyphenyl) propanoic acid (**10j**)*

White amorphous solid (80% yield); ^{1}H NMR ($CDCl_3$, 300 MHz): δ (ppm), 3.09–3.22 (m, 2H, CH_2), 3.84 (s, 3H, OCH_3), 3.85 (s, 3H, OCH_3), 4.66 (s, 2H, CH_2), 5.22–5.26 (m, 1H, CH), 6.26 (d, J = 16.2 Hz, 1H, CH), 6.65–6.93 (m, 5H, ArH), 7.26–7.49 (m, 7H, ArH), 7.56 (d, J = 15.9 Hz, 1H, CH); ^{13}C NMR ($CDCl_3$, 75 MHz): δ (ppm), 37.0, 55.9, 71.0, 71.2, 73.0, 112.2, 113.3, 114.4, 115.6, 117.2, 121.5, 122.7, 127.9, 129.9, 144.3, 145.3, 146.0, 146.4, 148.7, 165.7, 168.1; ESI-MS: m/z 463.2 $[M + H]^+$, 485.3 $[M + Na]^+$, 461.0 $[M - H]^-$; HRMS (ESI): m/z calcd for $C_{27}H_{26}O_7$ Na $[M + Na]^+$: 485.1576, found 485.1568.

*5.1.12. (E)-3-(3,4-dimethoxyphenyl)-2-(3-(4-methoxyphenyl) acryloyloxy) propanoic acid (**10k**)*

Yellow white solid (80% yield); ^{1}H NMR ($CDCl_3$, 300 MHz): δ (ppm), 3.04–3.22 (m, 2H, CH_2), 3.77 (s, 3H, OCH_3), 3.81 (s, 3H, OCH_3), 3.82 (s, 3H, OCH_3), 5.28(brs, 1H, CH), 6.27 (d, J = 15.9 Hz, 1H, CH), 6.72–6.84 (m, 5H, ArH), 7.36 (d, J = 8.7 Hz, 2H, ArH), 7.58 (d, J = 15.9 Hz, 1H, CH); ^{13}C NMR ($CDCl_3$, 75 MHz): δ (ppm), 37.0, 55.8, 55.9, 73.2, 111.2, 112.6, 118.8, 121.6, 128.3, 129.2, 130.9, 131.8, 134.7, 146.3, 148.4, 148.9, 166.7, 168.8; ESI-MS: m/z 409.3 $[M + Na]^+$, 385.0 $[M - H]^-$; HRMS (ESI): m/z calcd for $C_{21}H_{22}O_7$Na $[M + Na]^+$: 409.1263, found 409.1285.

*5.1.13. (E)-2-(3-(3,4-dihydroxyphenyl) acryloyloxy)-3-(3,4-dimethoxyphenyl) propanoic acid (**10l**)*

White amorphous solid (77% yield); ^{1}H NMR ($CDCl_3$, 300 MHz): δ (ppm), 3.11–3.28 (m, 2H, CH_2), 3.70 (s, 3H, OCH_3), 3.73 (s, 3H, OCH_3), 5.10–5.24 (m, 1H, CH), 6.25 (d, J = 15.9 Hz, 1H, CH), 6.75–7.05 (m, 6H, ArH), 7.47 (d, J = 15.9 Hz, 1H, CH); ^{13}C NMR ($CDCl_3$, 75 MHz): δ (ppm), 37.1, 55.9, 73.3, 113.9, 114.7, 115.3, 115.9, 116.3, 121.1, 122.0, 127.1, 128.9, 143.0, 144.1, 145.2, 145.9, 148.0, 166.2, 167.9; ESI-MS: m/z 411.3 $[M + Na]^+$, 387.0 $[M - H]^-$; HRMS (ESI): m/z calcd for $C_{20}H_{20}O_8$Na $[M + Na]^+$: 411.1056, found 411.1034.

*5.1.14. (E)-3-(3,4-dimethoxyphenyl)-2-(3-(3,4-dimethoxyphenyl) acryloyloxy) propanoic acid (**10m**)*

White amorphous solid (85% yield); ^{1}H NMR ($CDCl_3$, 300 MHz): δ (ppm), 3.07–3.21 (m, 2H, CH_2), 3.84 (s, 3H, OCH_3), 3.86 (s, 3H, OCH_3), 3.90 (s, 3H, OCH_3), 3.91 (s, 3H, OCH_3), 5.32–5.38 (m, 1H, CH), 6.34 (d, J = 15.9 Hz, 1H, CH), 6.77–6.98 (m, 4H, ArH), 7.11–7.24 (m, 2H, Ar), 7.64 (d, J = 15.9 Hz, 1H, CH); ^{13}C NMR ($CDCl_3$, 75 MHz): δ (ppm), 37.1, 55.8, 55.9, 73.0, 111.2, 111.5, 112.6, 114.6, 118.8, 121.5, 122.9, 128.4, 131.5, 146.0, 148.1, 148.8, 149.3, 151.4, 166.1, 167.6; ESI-MS: m/z 439.1 $[M + Na]^+$, 415.0 $[M - H]^-$; HRMS (ESI): m/z calcd for $C_{22}H_{24}O_8$Na $[M + Na]^+$: 439.1369, found 439.1351.

*5.1.15. (E)-2-(3-(3,4-bis (benzyloxy) phenyl) acryloyloxy)-3-(3,4-dimethoxyphenyl) propanoic acid (**10n**)*

White amorphous solid (81% yield); ^{1}H NMR ($CDCl_3$, 300 MHz): δ (ppm), 3.04–3.33 (m, 2H, CH_2), 3.82 (s, 3H, OCH_3), 3.84 (s, 3H, OCH_3), 5.15 (s, 2H, CH_2), 5.18 (s, 2H, CH_2),5.35 (s, 1H, CH), 6.26 (d, J = 15.9 Hz, 1H, CH), 6.75–7.61 (m, 18H, ArH and CH); ^{13}C NMR ($CDCl_3$, 75 MHz): δ (ppm), 36.9, 55.9, 71.1, 71.3, 72.9, 111.2, 112.7, 113.6, 114.4, 114.9, 121.6, 122.0, 123.3, 123.8, 127.2, 127.5, 128.1, 128.8, 136.9, 148.3, 149.2, 165.7, 168.1; ESI-MS: m/z 569.2 $[M + H]^+$, 591.3 $[M + Na]^+$; HRMS (ESI): m/z calcd for $C_{34}H_{32}O_8$Na $[M + Na]^+$: 591.1995, found 591.1979.

*5.1.16. (E)-3-(3,4-dimethoxyphenyl)-2-(3-(naphthalen-2-yl) acryloyloxy) propanoic acid (**10o**)*

White amorphous solid (88% yield); ^{1}H NMR ($CDCl_3$, 300 MHz): δ (ppm), 3.05–3.19 (m, 2H, CH_2), 3.79 (s, 3H, OCH_3), 3.82 (s, 3H, OCH_3), 5.34 (d, 1H, J = 6.8 Hz, CH), 6.56 (d, J = 15.6 Hz, 1H, CH), 6.72 (d, J = 7.8 Hz, 1H, ArH), 6.84 (d, J = 10.2 Hz, 2H, ArH), 7.47–7.51 (m, 2H, ArH), 7.57 (d, J = 8.7 Hz, 1H, CH), 7.74–7.82 (m, 5H, ArH and CH); ^{13}C NMR ($CDCl_3$, 75 MHz): δ (ppm), 37.1, 55.9, 73.1, 111.3, 112.7, 118.3, 121.6, 123.5, 126.8, 127.4, 127.8, 128.5, 128.8, 130.2, 131.7, 133.5, 146.3, 148.3, 148.9, 166.7, 168.1; ESI-MS: m/z 429.3 $[M + Na]^+$, 405.0 $[M - H]^-$; HRMS (ESI): m/z calcd for $C_{24}H_{22}O_6$Na $[M + Na]^+$: 429.1314, found 429.1341.

*5.1.17. (E)-2-(3-(2,3-dihydrobenzofuran-6-yl) acryloyloxy)-3-(3,4-dimethoxyphenyl) propanoic acid (**10p**)*

White amorphous solid (83% yield); ^{1}H NMR ($CDCl_3$, 300 MHz): δ (ppm), 3.08–3.24 (m, 4H, CH_2), 3.85 (s, 3H, OCH_3), 3.86 (s, 3H, OCH_3), 4.62 (t, J = 8.7 Hz, 2H, CH_2), 5.32–5.36 (m, 1H, CH), 6.29 (d, J = 15.9 Hz, 1H, CH), 6.76–6.83 (m, 4H, ArH), 7.37 (s, 1H, ArH), 7.63 (d, J = 15.9 Hz, 1H, CH); ^{13}C NMR ($CDCl_3$, 75 MHz): δ (ppm), 29.7, 37.1, 55.8, 71.9, 72.7, 109.7, 111.1, 112.7, 112.9, 121.7, 124.7, 126.7, 127.9, 128.2, 130.0, 146.9, 148.0, 148.7, 162.8, 165.9, 167.0; ESI-MS: m/z 421.3 $[M + Na]^+$, 397.0 $[M - H]^-$; HRMS (ESI): m/z calcd for $C_{22}H_{22}O_7$Na $[M + Na]^+$: 421,1263, found 421,1242.

*5.1.18. Typical reaction procedure for compounds (**11f**, **11i**, **11j**, and **11n**–**p**)*

A solution of Dicyclohexylcarbodiimide (DCC) (0.12 mmol), 4-dimethylaminopyridine (DMAP) (0.01 mmol), acid **10f**, **i**, **j**, or **n**–**p** (0.1 mmol), and CH_2Cl_2 (10 mL) was stirred at 0 °C for 15 min. After addition of hydroxylamine hydrochloride ($NH_2OH{\cdot}HCl$) (0.12 mmol), the mixture was stirred at room temperature for 24 h. The organic layers were washed with water after filtration, concentrated under reduced pressure. The crude material was chromatographed on SiO_2 (petroleum ether and ethyl acetate (6:4) as eluent) to afford **11f**, **11i**, **11j**, or **11n**–**p**.

*5.1.19. (E)-3-(3,4-dimethoxyphenyl)-1-(hydroxyamino)-1-oxopropan-2-yl 3-(4-bromophenyl) acrylate (**11f**)*

White power (60% yield); ^{1}H NMR ($CDCl_3$, 300 MHz): δ (ppm), 3.14–3.28 (m, 2H, CH_2), 3.84 (s, 3H, OCH_3), 3.86 (s, 3H, OCH_3), 5.52 (brs, 1H, CH), 6.38 (d, J = 16.2 Hz, 1H, CH), 6.71–6.79 (m, 3H, ArH), 7.34 (d, J = 8.1 Hz, 2H, ArH), 7.52 (d, J = 8.1 Hz, 2H, ArH), 7.60 (d, J = 15.9 Hz, 1H, CH); ^{13}C NMR ($CDCl_3$, 75 MHz): δ (ppm), 37.0, 55.9, 72.9, 111.2, 112.6, 117.0, 117.7, 121.7, 125.4, 129.6, 132.2, 144.7, 145.6, 148.2, 148.9, 165.2, 166.7; ESI-MS: m/z 474.1 $[M + Na]^+$, 449.9 $[M - H]^-$, 898.9 $[2M - H]^-$; HRMS (ESI): m/z calcd for $C_{20}H_{20}BrNO_6$Na $[M + Na]^+$: 472.0372, found 472.0394.

*5.1.20. (E)-3-(3,4-dimethoxyphenyl)-1-(hydroxyamino)-1-oxopropan-2-yl 3-(4-phenylphenyl) acrylate (**11i**)*

White power (66% yield); ^{1}H NMR ($CDCl_3$, 300 MHz): δ (ppm), 3.08–3.22 (m, 2H, CH_2), 3.84 (s, 3H, OCH_3), 3.86 (s, 3H, OCH_3), 5.57 (brs, 1H, CH),6.49 (d, J = 15.6 Hz, 1H, CH), 6.67–7.86 (m, 3H, ArH), 7.35–7.70 (m, 9H, ArH), 7.76 (d, J = 15.9 Hz, 1H, CH); ^{13}C NMR ($CDCl_3$, 75 MHz): δ (ppm), 37.1, 55.9, 73.1, 111.3, 112.8, 116.9, 121.9, 127.5, 127.9, 128.2, 128.7, 128.9, 129.3, 132.9, 140.1, 143.6, 145.9, 148.5, 148.9, 166,4, 167.7; ESI-MS: m/z 470.3 $[M + Na]^+$, 446.1 $[M - H]^-$; HRMS (ESI): m/z calcd for $C_{26}H_{25}NO_6$Na $[M + Na]^+$: 470.1580, found 470.1561.

*5.1.21. (E)-3-(3,4-dimethoxyphenyl)-1-(hydroxyamino)-1-oxopropan-2-yl 3-(4-(benzyloxy) phenyl) acrylate (**11j**)*

White power (50% yield); ^{1}H NMR ($CDCl_3$, 300 MHz): δ (ppm), 3.15–3.29 (m, 2H, CH_2), 3.83 (s, 3H, OCH_3), 3.86 (s, 3H, OCH_3), 5.13 (s, 2H, CH_2), 5.57 (brs, 1H, CH), 6.28 (d, J = 15.6 Hz, 1H, CH), 6.72–

6.81 (m, 3H, ArH), 6.99 (d, J = 8.4 Hz, 2H, ArH), 7.41–7.51 (m, 7H, ArH), 7.65 (d, J = 15.9 Hz, 1H, CH); ^{13}C NMR ($CDCl_3$, 75 MHz): δ (ppm), 37.1, 55.9, 71.2, 71.3, 73.2, 112.3, 113.7, 114.5, 115.6, 117.5, 121.6, 122.7, 127.9, 129.6, 144.5, 145.3, 146.1, 146.7, 148.9, 166.1, 168.3; ESI-MS: m/z 500.2 $[M + Na]^+$, 476.1 $[M - H]^-$; HRMS (ESI): m/z calcd for $C_{27}H_{27}NO_7Na$ $[M + Na]^+$: 500.1685, found 500.1669.

*5.1.22. (E)-3-(3,4-dimethoxyphenyl)-1-(hydroxyamino)-1-oxopropan-2-yl 3-(3,4-bis (benzyloxy) phenyl) acrylate (**11n**)*

White power (53% yield); ^{1}H NMR ($CDCl_3$, 300 MHz): δ (ppm), 3.09–3.31 (m, 2H, CH_2), 3.81 (s, 3H, OCH_3), 3.84 (s, 3H, OCH_3), 5.18 (s, 2H, CH), 5.20 (s, 2H, CH), 5.54 (s, 1H, CH), 6.20 (d, J = 15.9 Hz, 1H, CH), 6.71–6.79 (m, 3H, ArH), 6.92 (d, J = 8.1 Hz, 1H, ArH), 7.01–7.17 (m, 2H, ArH), 7.30–7.52 (m, 10H, ArH), 7.56 (d, J = 15.9 Hz, 1H, CH); ^{13}C NMR ($CDCl_3$, 75 MHz): δ (ppm), 36.8, 55.9, 71.0, 71.4, 72.8, 107.6, 108.7, 111.2, 112.7, 113.9, 114.2, 114.7, 121.6, 121.8, 123.3, 123.5, 127.2, 127.3, 128.0, 128.6, 136.8, 148.2, 149.0, 165.6, 167.9; ESI-MS: m/z 606.3 $[M + Na]^+$, 582.1 $[M - H]^-$; HRMS (ESI): m/z calcd for $C_{34}H_{33}NO_8Na$ $[M + Na]^+$: 606.2104, found 606.2095.

*5.1.23. (E)-3-(3,4-dimethoxyphenyl)-1-(hydroxyamino)-1-oxopropan-2-yl 3-(naphthalene-2-yl) acrylate (**11o**)*

White power (58% yield); ^{1}H NMR ($CDCl_3$, 300 MHz): δ (ppm), 3.09–3.24 (m, 2H, CH_2), 3.84 (s, 3H, OCH_3), 3.86 (s, 3H, OCH_3), 5.58 (brs, 1H, CH), 6.50 (d, J = 15.6 Hz, 1H, CH), 6.69–6.82 (m, 3H, ArH), 7.50–7.84 (m, 8H, ArH and CH); ^{13}C NMR ($CDCl_3$, 75 MHz): δ (ppm), 37.0, 55.9, 73.1, 111.2, 112.6, 118.5, 121.7, 123.9, 126.7, 127.7, 127.9, 128.3, 128.8, 130.3, 131.9, 133.7, 146.1, 148.2, 148.7, 165.8, 167.5; ESI-MS: m/z 444.3 $[M + Na]^+$, 420.0 $[M - H]^-$; HRMS (ESI): m/z calcd for $C_{24}H_{23}NO_6Na$ $[M + Na]^+$: 444.1423, found 444.1409.

*5.1.24. (E)-3-(3,4-dimethoxyphenyl)-1-(hydroxyamino)-1-oxopropan-2-yl 3-(2,3-dihydrobenzofuran-6-yl) acrylate (**11p**)*

White power (69% yield); ^{1}H NMR ($CDCl_3$, 300 MHz): δ (ppm), 3.09–3.27 (m, 4H, CH_2), 3.82 (s, 3H, OCH_3), 3.84 (s, 3H, OCH_3), 4.62 (t, J = 8.7 Hz, 2H, CH_2), 5.53 (brs, 1H, CH), 6.24 (d, J = 15.6 Hz, 1H, CH), 6.73–6.80 (m, 4H, ArH), 7.30–7.37 (m, 2H, ArH), 7.63 (d, J = 15.9 Hz, 1H, CH); ^{13}C NMR ($CDCl_3$, 75 MHz): δ (ppm), 29.5, 37.0, 55.8, 71.8, 72.8, 109.9, 111.2, 112.7, 112.8, 121.6, 124.8, 126.5, 127.4, 128.7, 130.3, 146.7, 148.3, 148.9, 162.2, 165.6, 166.7; ESI-MS: m/z 436.2 $[M + Na]^+$, 412.0 $[M - H]^-$; HRMS (ESI): m/z calcd for $C_{22}H_{23}NO_7Na$ $[M + Na]^+$: 436.1372, found 436.1395.

5.2. MMP-1 inhibition assay

The catalytic domain of human MMP-1 was purchased from AnaSpec. The protease activity of MMP-1 was measured by using a quenched fluorogenic peptide substrate: Dnp-Pro-beta-cyclohexyl-Ala–Gly–Cys(Me)–His–Ala–Lys(Nma)-NH_2 (Biomol USA). MMP-1 activity assay was performed in a 96-well plate in a total assay volume of 200 μL. The recombinant MMP-1 (30 nM) was incubated for 30 min at room temperature in reaction buffer (50 mM Tris-HCl, 150 mM NaCl, 10 mM $CaCl_2$, 0.05% Brij-35, pH 7.5) with different concentrations of the compounds to be tested. Compounds solutions were prepared from stock in DMSO. After 20 min incubation at room temperature, the substrate was added to a final concentration of 5 μM. Fluorescence intensities (Ex/Em = 340/440 nm) were monitored for 60 min at room temperature with a Synergy™2 Multi-Mode Microplate Reader (BioTek). IC_{50} values were calculated using the GraphPad Prism software with three independent determinations.

5.3. Molecular docking

The crystal structure of MMP-1 was retrieved from the Protein Data Bank (PDB entry: 966C), and all water molecules were removed from the complex structure. Hydrogen atoms and charges were added during a brief relaxation performed using the "Protein Preparation Wizard" workflow in Maestro 9.0. After optimizing the hydrogen bond network, the crystal structure was minimized using OPLS 2005 force field with the maximum RMSD value of 0.3 Å. The grid-enclosing box was centered on the ligand in the refined crystal structure as described above and defined so as to enclose residues located within 14 Å from the ligand, and a scaling factor of 1.0 was set to van der Waals (VDW) radii with the partial atomic charges of 0.25 to soften the nonpolar parts of the receptor. And the three-dimensional structures of compounds were generated with Ligprep module. In the docking process, standard precision (SP) and extra precision (XP) approaches were adopted successively, and the top 10 conformations were retrieved and ranked by GlideScore with the XP mode, while these conformations were visually inspected for their binding modes. Finally, the most reasonable conformation was selected for explaining the structure activity relationship of inhibitor against MMP-1.

Additional experimental details and NMR (^{1}H and ^{13}C), ESI-MS and HRMS spectra of compounds has been included in the Supporting information.

Acknowledgment

The work was supported by program NCET Foundation, NSFC (30725045), partially supported by Global Research Network for Medicinal Plants (GRNMP) and King Saud University, Shanghai Leading Academic Discipline Project(B906), FP7- PEOPLE-IRSES-2008 (TCMCANCER Project 230232), Key laboratory of drug research for special environments, PLA, Shanghai Engineering Research Center for the Preparation of Bioactive Natural Products(10DZ2251300) and the Scientific Foundation of Shanghai China (09DZ1975700, 09DZ1971500,10DZ1971700). The MMP-1 expression plasmid was kindly provided by Prof. Zigang Dong, University of Minnesota.

Appendix A. Supporting information

Supporting information related to this article can be found at http://dx.doi.org/10.1016/j.ejmech.2012.09.047.

References

[1] J. Huxley-Jones, S.M. Foord, M.R. Barnes, Drug Discov. Today 13 (2008) 685–694.
[2] M. Hidalgo, S.G. Eckhardt, J. Natl. Cancer Inst. 93 (2001) 178–193.
[3] H.I. Roach, Expert Opin. Drug Discov. 3 (2008) 475–486.
[4] L. Dahlberg, R.C. Billinghurst, P. Manner, F. Nelson, G. Webb, M. Ionescu, A. Reiner, M. Tanzer, D. Zukor, J. Chen, Arthritis Rheum. 43 (2000) 673–682.
[5] U. Ikeda, K. Shimada, Clin. Cardiol. 26 (2003) 55–59.
[6] B.K. Pilcher, M. Wang, X.J. Qin, W.C. Parks, R.M. Senior, H.G. Welgus, Ann. N.Y. Acad. Sci. 878 (1999) 12–24.
[7] A.D. Rowan, G.J. Litherland, W. Hui, J.M. Milner, Expert Opin. Ther. Targets 12 (2008) 1–18.
[8] B. Fingleton, Curr. Pharm. Des. 13 (2007) 333–346.
[9] S. Lefèvre, A. Knedla, C. Tennie, A. Kampmann, C. Wunrau, R. Dinser, A. Korb, E.M. Schnker, I.H. Tarner, P.D. Robbins, Nat. Med. 15 (2009) 1414–1420.
[10] I. Rush, S. Thomas, R. Powers, Curr. Top. Med. Chem. 4 (2004) 1311–1327.
[11] R.P. Verma, C. Hansch, Bioorg. Med. Chem. 15 (2007) 2223–2268.
[12] J. Gross, C.M. Lapiere, Proc. Natl. Acad. Sci. U. S. A. 48 (1962) 1014.
[13] M.D. Sternlicht, Z. Werb, Annu. Rev. Cell. Dev. Biol. 17 (2001) 463.
[14] M. Egeblad, Z. Werb, Nat. Rev. Cancer 2 (2002) 161–174.
[15] W.C. Parks, C.L. Wilson, Y.S. López-Boado, Nat. Rev. Immunol. 4 (2004) 617–629.
[16] I. Stamenkovic, J. Pathol. 200 (2003) 448–464.
[17] Z.S. Galis, J.J. Khatri, Circ. Res. 90 (2002) 251–262.
[18] T.S.P. Elkington, R. Breen, K.N. Robert, J. Clin. Invest. 121 (2011) 1827–1833.
[19] B. Lovejoy, A. Cleasby, A.M. Hassell, K. Longley, M. Luther, D. Weigl, G. McGeehan, A.B. McElroy, D. Drewry, M.H. Lambert, Science 263 (1994) 375.
[20] N. Borkakoti, F. Winkler, D. Williams, A. D'Arcy, M. Broadhurst, P. Brown, W. Johnson, E. Murray, Nat. (London) Struct. Biol. 1 (1994) 106–110.
[21] B. Lovejoy, A.R. Welch, S. Carr, C. Luong, C. Broka, R.T. Hendricks, J.A. Campbell, K.A.M. Walker, R. Martin, H.W. Van, Nat. Struct. Mol. Biol. 6 (1999) 217–221.

[22] M. Whittaker, C.D. Floyd, P. Brown, A.J.H. Gearing, Chem. Rev. 99 (1999) 2735–2776.
[23] B.G. .Rao, Curr. Pharm. Des. 11 (2005) 295–322.
[24] J.W. Skiles, N.C. Gonnella, A.Y. Jeng, Curr. Med. Chem. 11 (2004) 2911–2977.
[25] E. Rosenbaum, M. Zahurak, V. Sinibaldi, M.A. Carducci, R. Pili, M. Laufer, T.L. DeWeese, M.A. Eisenberger, Clin. Cancer Res. 11 (2005) 4437.
[26] D. Bissett, K.J. O'Byrne, J. Von Pawel, U. Gatzemeier, A. Price, M. Nicolson, R. Mercier, E. Mazabel, C. Penning, M.H. Zhang, J. Clin. Oncol. 23 (2005) 842.
[27] F. Hemmings, M. Farhan, J. Rowland, L. Banken, R. Jain, Rheumatology 40 (2001) 537.
[28] R. Paul Beckett, Expert Opin. Ther. Pat. 6 (1996) 1305–1315.
[29] C. Queffélec, F. Bailly, G. Mbemba, J.F. Mouscadet, Z. Debyser, M. Witvrouw, P. Cotelle, Eur. J. Med. Chem. 43 (2008) 2268–2271.
[30] H.N.C. Wong, Z.L. Xu, H.M. Chang, C.M. Lee, Synthesis 8 (1992) 793–797.
[31] H. Kunz, H. Waldmann, Angew. Chem. Int. Ed. 23 (1984) 71–72.
[32] J. Minamikawa, A. Brossi, Tetrahedron Lett. 34 (1978) 3085–3086.
[33] O.A.T. Donini, P.A. Kollman, J. Med. Chem. 43 (2000) 4180–4188.